The AAPS Journal, Vol. 12, No. 3, September 2010 (© 2010)
DOI: 10.1208/s12248-010-9204-2

Research Article

Theme: Fishing for the Hidden Proteome in Health and Disease: Focus on Drug Abuse
Guest Editors: Rao S. Rapaka, Lloyd D. Fricker, and Jonathan V. Sweedler

Mass Spectrometry Screening Reveals Peptides Modulated Differentially in the Medial Prefrontal Cortex of Rats with Disparate Initial Sensitivity to Cocaine

Elena V. Romanova,[1] Ji Eun Lee,[1] Neil L. Kelleher,[1] Jonathan V. Sweedler,[1,4] and Joshua M. Gulley[2,3,4]

Received 22 February 2010; accepted 3 May 2010; published online 19 May 2010

Abstract. To better understand why certain individuals are more vulnerable to cocaine abuse and addiction, we identify peptide markers associated with individual variation in sensitivity to the behavioral effects of cocaine. Previous studies in rats show that low, compared to high, cocaine responders are more sensitive to cocaine-induced behavioral plasticity (sensitization), exhibit enhanced conditioning to cocaine's rewarding effects, and are more motivated to self administer cocaine. In the current study, we combine matrix-assisted laser desorption/ionization mass spectrometry with multivariate statistical methods to analyze tissue extracts from rat dorsal striatum, nucleus accumbens, and medial prefrontal cortex (mPFC) to examine trends in peptide changes that coincide with behavioral phenotype. Peptide profiles of these three regions from individual animals were characterized via mass spectrometry. Resulting mass peaks that were statistically different between these groups were identified using principal component analysis. The mass peaks were then identified in pooled samples via multistage liquid chromatography mass spectrometry. A total of 74 peptides from 28 proteins were sequenced from defined brain regions. Statistically significant changes in peak intensities for seven peptides were found in the mPFC of rats given a single injection of 10 mg/kg cocaine, with low cocaine responders showing ~2-fold increase in peak intensities for the acetylated N terminus peptides of stathmin and Hint 1, as well as truncated ATP synthase. These results suggest that distinct peptide profiles in the mPFC are associated with individuals that exhibit reduced sensitivity to the behavioral effects of cocaine.

KEY WORDS: addiction; biomarkers; MALDI-TOF; peptidomics; principle component analysis.

INTRODUCTION

Efforts to determine the antecedents of addiction have revealed several factors that are predictive of long-term drug use and abuse. For example, individuals less sensitive to the intoxicating effects of ethanol are more sensitive to its properties that facilitate the transition to abuse and dependence (1). For psychostimulant drugs, a high degree of "liking" or "wanting" on initial use of cocaine is associated with a significantly increased risk of cocaine abuse (2). Rats and non-human primates also exhibit robust variability in their response to a number of cocaine's effects, including its cardiovascular effects (3), psychomotor-stimulant properties (4,5), capacity to produce behavioral sensitization (6,7), and its ability to reinforce operant behavior (8–10).

One reliable animal model that we and others have used to study individual differences in initial sensitivity is cocaine-induced locomotor activation in an open-field arena. Outbred male and female rats can readily be classified as low or high cocaine responders (LCRs or HCRs, respectively) based, correspondingly, on their relatively reduced or exaggerated response to a single treatment with cocaine (4,11–13). In additional studies of cocaine's effects in these phenotypes, it has been shown that, compared to HCRs, LCRs exhibit greater cocaine-induced locomotor sensitization following repeated cocaine exposure (14,15), an increased response to the rewarding properties of cocaine in a conditioned place preference paradigm (16), enhanced motivation to self-administer cocaine when the drug is delivered on a progressive ratio schedule of reinforcement (17), and greater sensitivity to the discriminative stimulus properties of cocaine (14). These results are consistent with the notion of LCRs as a more "vulnerable" phenotype in these rodent models of

Electronic supplementary material The online version of this article (doi:10.1208/s12248-010-9204-2) contains supplementary material, which is available to authorized users.

[1] Department of Chemistry and the Beckman Institute, University of Illinois at Urbana-Champaign, 600 S. Mathews Ave., Urbana, Illinois 61801, USA.
[2] Department of Psychology, University of Illinois at Urbana-Champaign, 603 E. Daniel St., Champaign, Illinois 61820, USA.
[3] Neuroscience Program, University of Illinois at Urbana-Champaign, 505 South Goodwin Avenue, Urbana, Illinois 61801, USA.
[4] To whom correspondence should be addressed. (e-mail: jsweedle@illinois.edu; jgulley@illinois.edu)

addiction-related behaviors. Previously, we demonstrated a role for phenotypic differences in 5-HT_{1A} and 5-HT_2 receptors in the disparate delay discounting (18) and cocaine discrimination behavior (14) observed between LCRs and HCRs. Sabeti *et al.* (4,15) found that cocaine-induced inhibition of dopamine transporter (DAT) activity in the dorsal striatum (dSTR) and nucleus accumbens (NAc) is significantly greater in HCRs compared to LCRs during the first cocaine exposure but that following repeated cocaine treatment the drug was equally effective at inhibiting transporter activity in both LCRs and HCRs. There is also evidence that DAT is more highly expressed in the dSTR and NAc of LCRs compared to HCRs (19) and that cocaine regulates the cell-surface expression of DAT differentially in these phenotypes (20,21).

A growing number of studies point to a role for peptide signaling in both the acute and long-term responses to cocaine (22–24). We sought to determine whether differences in initial sensitivity to cocaine are associated with changes in levels of detectable peptides in the dSTR, NAc, and medial prefrontal cortex (mPFC). Instead of preselecting candidate peptides to test, we employed matrix-assisted laser desorption/ionization (MALDI) time of flight (TOF) mass spectrometry (MS) profiling, in combination with principal component analysis (PCA), to enable global peptide/protein characterization and reveal the putative peptide markers linking neurochemical response to cocaine-induced behavior. Information-rich, compatible with small samples, and sensitive, MALDI-MS is shown to be useful for label-free, semiquantitative analysis of raw tissue extracts, primarily due to its high tolerance to salts, and small-volume sample requirements (23,25–27).

It is important to note that the measurements described here are performed on individual rather than pooled samples; thus, the peptide profiles are directly compared with an individual's behavioral responses using PCA of our MS data. There exist inherent challenges to this approach. For example, when performing individual measurements, only small amounts of material are obtained, and larger numbers of samples are required. Often, fast postmortem protein degradation can overwhelm low abundance species, such as bioactive peptides. Moreover, a discrepancy is created when a large number of samples are required to achieve ideal statistical analyses, but there are only a limited number of individual tissue samples available. Fortunately, our recently reported peptide extraction method ameliorates some of these deleterious effects by allowing simultaneous peptide extraction and preservation of tissue samples for future analyses (28). We validate this approach by comparing the spectra from specific, anatomically defined brain regions in individual animals to uncover changes in peptides that distinguish naïve and drug-exposed rats with differing sensitivities to cocaine-induced behavior.

MATERIALS AND METHODS

Animals

Male Sprague–Dawley rats (n=24), bred in our animal facility from stock rats obtained from Harlan, were housed individually starting at ~2 months of age and were 2.5–3 months old at the start of experiments. Animals were maintained on a 12:12 h light–dark cycle (lights on at 0800 hours) with food and water available *ad libitum*. Prior to being used in the study, rats were handled on five separate occasions for 15 min. All experimental procedures were approved by the IACUC at the University of Illinois, Urbana-Champaign and were consistent with the *Principles of Laboratory Animal Care* (NIH Publication no. 85-23).

Assessment of Locomotor Activity

Tests of saline- and cocaine-induced changes in locomotor activity were performed in four open-field activity chambers. On the day of testing, rats were brought to the procedure room and allowed to acclimate to the environment for 30 min. They were then placed individually into an open-field chamber for 90 min; 10 rats were randomly assigned to receive saline and the remaining 14 were given cocaine. Each animal was removed and injected (i.p.) with saline (1 ml/kg) or (−) cocaine HCl (10 mg/kg) and placed back into the chamber for an additional 30 min. The dose of cocaine was chosen based on previous studies (4,11,12) showing that it is optimal for inducing the widest range of behavioral responses in male Sprague–Dawley rats. Animals were characterized as LCRs or HCRs by analyzing cumulative activity data for 30 min following injection. As in previous studies (11,12), rats with activity scores in the lower half of the population distribution were designated LCRs, and those in the upper half were designated HCRs. The statistical significance of group differences in activity following injection (saline or cocaine) was determined using one-way ANOVA followed by *post hoc* Tukey tests.

Tissue Sampling and Extraction of Peptides

Immediately following their removal from the open-field arena, rats were euthanized by rapid decapitation. Their brains were carefully removed, rinsed in ice-cold 0.9% saline, sliced in 2-mm coronal sections with the assistance of a calibrated brain matrix, and placed on a glass dish kept on ice. Within 1.5–3 min after decapitation, samples of the mPFC, NAc, and dSTR were isolated from these slices via biopsy punches of different diameters (0.75 mm mPFC; 1.2 mm NAc; 2.0 mm dSTR). While locomotor activity was measured in 10 rats after saline injection and 14 rats after cocaine (n=7 each for LCRs and HCRs), only a subset of these rats was used from each of the groups for MS analysis due to the high number of samples to process (as all samples were processed individually). Specifically, a total of 72 tissue samples (12 rats × 3 brain regions × 2 hemispheres) were obtained from the three groups of rats tested in the behavioral portion of the study (saline, LCR and HCR; n=4/group). For peptide extraction, tissue samples from each hemisphere were placed respectively in 10-, 15-, or 20-μL volumes of 2,5-dihydroxybenzoic acid (DHB: 20 mg/mL) and incubated for 48 h as described by Romanova *et al.* (28).

Analysis of Peptide Profiles by MALDI-TOF MS

Tissue samples from four rats of each group (saline-treated, LCRs, and HCRs) were used for MALDI MS

analysis. First, 0.7 μL of DHB extraction solution was spotted on a stainless steel MALDI target and co-crystallized with 0.7 μL of freshly prepared concentrated DHB matrix (50 mg/mL, in a 50% water/acetone mix). Positive ion mass spectra for three technical replicates of each tissue sample were acquired manually in the 600–6,000 *m/z* region using a Bruker Ultraflex II mass spectrometer (Bruker Daltonics) in reflectron mode with high-precision calibration.

Statistical analysis of raw MALDI MS data was performed using an evaluation version of ClinProTools software (Bruker Daltonics). Spectra were normalized to total ion count; peaks were selected based on maximal peak intensity in the mean spectrum from each sample group. Peptide profiles of mean spectra were compared by PCA followed by the Anderson–Darling normality test and *t* test or ANOVA for normal distributed data. Data not showing normal distribution ($p_{AD} \leq 0.05$) were evaluated by Wilcoxon or Kruskal–Wallis tests, respectively (29–31). To decrease the number of false positives while computing individual peak statistics on the complex spectra, the Benjamini–Hochberg procedure incorporated into ClinProTools was automatically applied for *p* value adjustment during analysis (32).

Identification of Peptides by LC-MS

Following MALDI MS profiling, the peptide extracts were pooled together. A significant portion of the DHB was removed from the extracts by solid-phase extraction (SPE) prior to multistage reversed phase (RP)–liquid chromatography (LC) separation of peptides. Peptides were sequenced by tandem mass spectrometry (MS/MS) using an HCT Ultra-PTM Discovery system ion-trap mass spectrometer (Bruker Daltonics) equipped with an electrospray ionization (ESI) source. Fragmentation spectra were analyzed against the NCBI and MSDS protein databases using Biotools 3.0 (Bruker Daltonics) and the Mascot server (Matrix Science) within Rattus taxonomy. Only peptides identified with ion scores that fell within the significance threshold of 0.05 are reported. For identifying peptides related to known prohormones, database searching was repeated on fragmentation peak lists exported in the form of a Mascot generic file format (mgf) against an in-house database of rat peptide prohormones using Peaks Studio 4.6 (Bioinformatics Solutions). Subsequently, the search results were verified by manual *de novo* analysis using Data Analysis 4.0 and Biotools 3.0 (Bruker Daltonics). Larger peptides were sequenced using a 12 Tesla LTQ-FT Ultra mass spectrometer (ThermoFisher Scientific). Fragmentation spectra were searched in a "neuropeptide" search mode against an intact rat database (UniProt 15.0, 4318021 protein forms) using ProSightPC 2.0 (ThermoFisher Scientific).

Additional experimental procedures and details are available in the Electronic Supplementary Material, including on the open-field activity chambers, the protocols for peptide analysis by MALDI-TOF MS, approaches for statistical analysis of the MALDI MS data, and SPE purification of the extracts.

RESULTS

Cocaine-Induced Behavior

As shown in Fig. 1a, rats initially responded to the novel open-field arena with significant exploratory activity that decreased within the first 45 min. Following injection of either saline or cocaine, activity increased but stayed high in only those rats given cocaine. More specifically, statistically significant increases in cocaine-induced behavior were seen only in rats classified as HCRs; LCRs did not differ significantly from rats injected with saline (Fig. 1b).

Classification of Brain Regions According to Peptide Profiles by MALDI-TOF MS and PCA

Recently we reported a one-step sample preparation approach by placing the tissue sample directly into the MALDI matrix, DHB, for effective extraction of peptides from brain tissue with prolonged incubations (28). Using this method, we profiled and compared individual 1.5–4 mm^3 samples of defined brain regions. Substantially overlapping but not identical sets of putative peptide peaks were detected in three defined regions of the brain reward circuit, the mPFC, NA, and dSTR (Fig. 2). To identify major peptide trends among these samples, we applied PCA to the normalized MS data (Fig. 3). The results improved by restricting the peptide peaks considered for PCA to 50,

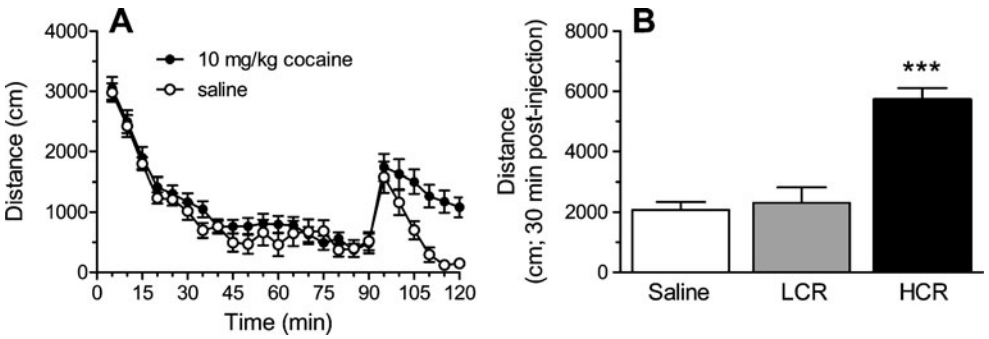

Fig. 1. The effects of saline or cocaine on locomotor activity in an open-field arena. Injections were given 90 min after rats were put into the arena for the first time. **A** Time course showing activity in 5-min bins for 90 min before and 30 min after injection with saline ($n=10$) or 10 mg/kg cocaine ($n=14$). **B** Cumulative activity is shown for the 30-min following saline or cocaine injection. Rats given cocaine were characterized as LCRs or HCRs ($n=7$/group) if their response fell below or above, respectively, the median value for the population (see "Materials and Methods" for details of characterization). *** $p<0.001$, compared to LCRs and to saline-treated rats

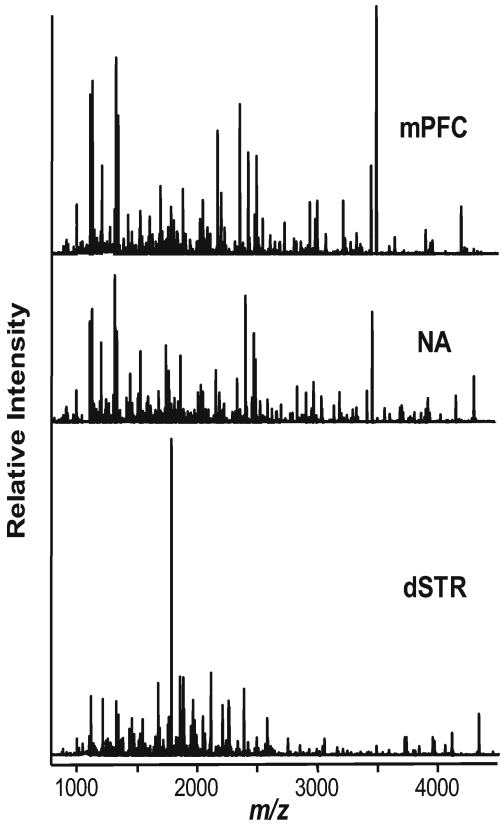

Fig. 2. MALDI MS spectra show highly overlapping but distinct peptide profiles in extracts from the brain regions in the control group of rats. *dSTR* dorsal striatum, *NA* nucleus accumbens, *mPFC* medial prefrontal cortex

selected according to signal-to-noise ratio and intensity. The dataset exhibited a degree of variability that required six main principal components (PCs) to describe the data. However, ~80% of the variation is accounted for by PC1 and <10% by PC2. Analysis of all six types of spectra (2 groups × 3 brain regions each) revealed no detectable change in the peptide profiles of dSTR after acute cocaine administration, as both control and cocaine samples tended to cluster on the PC plot (Fig. 4a). The NA samples, in contrast, showed a high dispersion along the PC3 coordinate on the PC plot following cocaine treatment, which contributes about 5% of the variability between the NA samples (Fig. 4b). A striking difference is found for mPFC samples from the cocaine-treated group. As shown on the PC plots in Fig. 5, the peptide profiles of cocaine-treated samples are clearly segregated from the control samples, and according to both PC1 and PC2. Loading plots highlight a subset of peptides that contribute to the changes in profiles and allow control and cocaine-treated groups to be distinguished biochemically (Fig. 5c). These results demonstrate the DHB extraction method to be simple, convenient, and useful for qualitative and semiquantitative comparisons of peptide profiles. The mass peaks differentially detected among brain regions by MALDI MS and selected by PCA and ANOVA tests have yet to be identified. These masses were then used in follow-up LC-MS/MS experiments using the remaining tissue extracts, which were then pooled as described below.

Identification of Peptides by LC-MS/MS

To identify peptides of interest, we extended our previous work (28) by interfacing the DHB extraction procedure to a separation method, but first, we needed to address some issues. First, the large excess of DHB relative to the peptides present in the extracts presents challenges in ESI-MS. In addition, DHB is known to co-migrate with polar peptides of 500–1,500*m/z* in RP-LC analysis (33). To address this analytical challenge, we opted to use an anionic ion-pairing agent, heptafluorobutyric acid (HFBA) and developed a multistage LC separation protocol, aided by prior SPE treatment of the extracts to remove the DHB prior to MS sequencing. HFBA is known to aid in the separation of peptides by their charge groups as well as their hydrophobicity within these groups (34). It also increases the retention time of peptides when compared to using trifluoroacetic acid (TFA). In addition, HFBA is less volatile than TFA, which can be an issue for ESI-MS. A drawback of the HFBA system, however, is peak broadening, which could limit the analysis of complex peptide samples. Thus, we

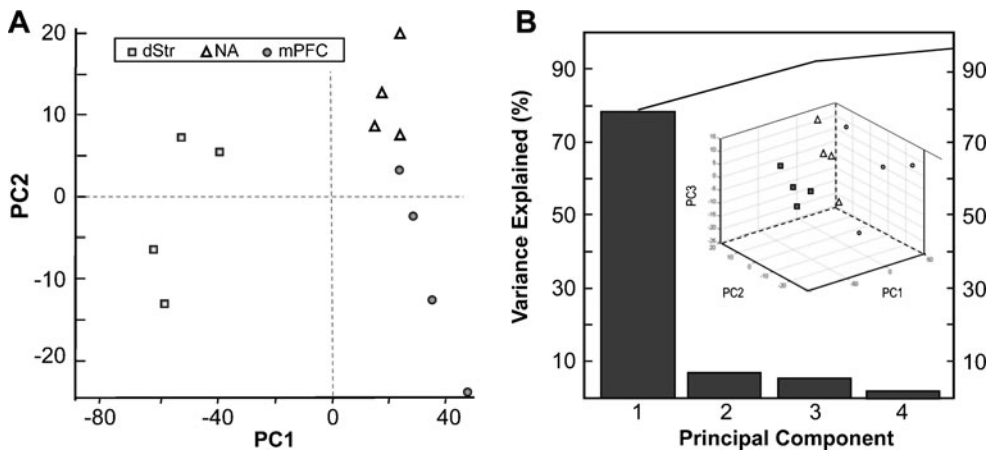

Fig. 3. PCA of normalized MS data. **A** PC score graph for the control group demonstrates the segregation of brain regions according to peptide profile. **B** Contribution of PCs constituting 95% of variance and 3D score plot are shown

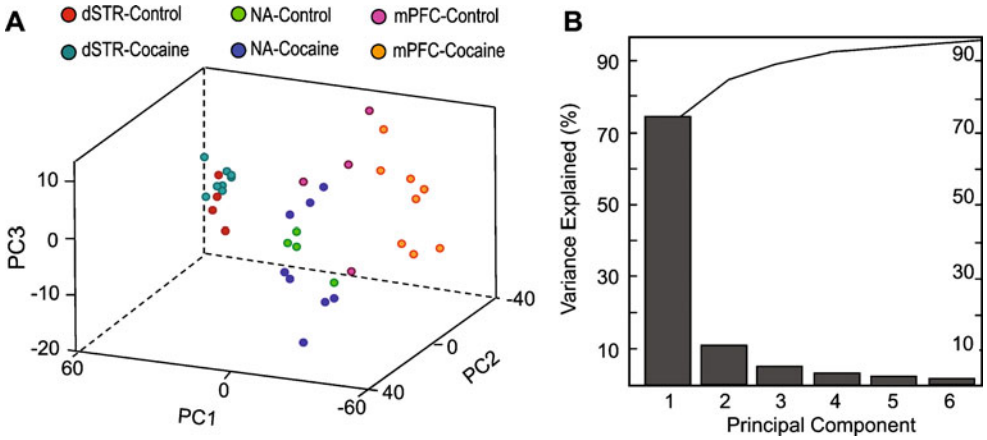

Fig. 4. PCA of MS data normalized to total ion count. **A** PC score graph for control and acute cocaine groups demonstrate segregation of brain regions according to the peptide profiles between control and cocaine treated groups. Each data point represents an individual sample. The mPFC extracts from control and cocaine-treated animals are clearly distinguished on the basis of their peptide profiles. **B** Contribution of PCs constituting 95% of variance

applied a second dimension to the RP-LC. First, we used the ACN/H_2O/HFBA solvent system (see Supplementary Material) and afterwards an aqueous MeOH gradient in the presence of formic acid that was compatible with online ESI-MS. The use of HFBA during SPE and the 1st stage LC separation allowed us to remove excess DHB from the extracts and purify a substantial number of peptides for sequencing (Fig. 6).

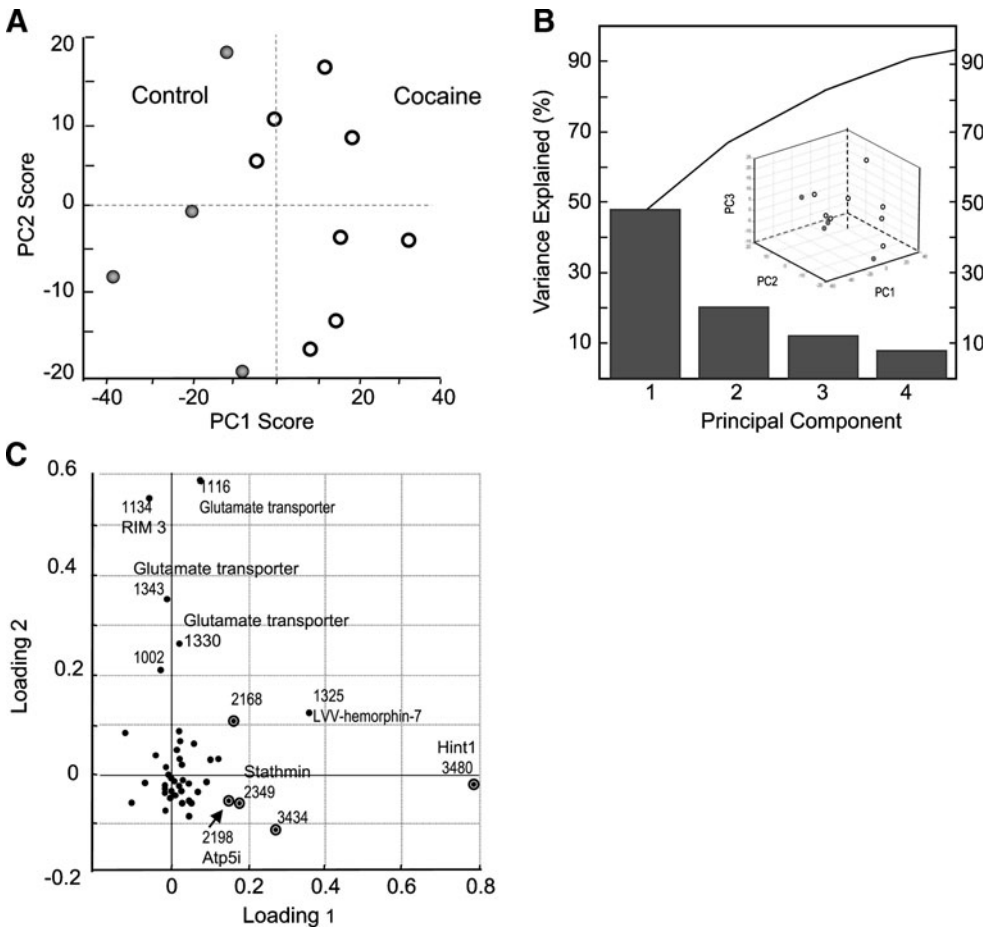

Fig. 5. PCA of MS data demonstrate that **A** samples of mPFC extracts from control and cocaine-treated animals can be distinguished on the basis of their peptide profiles. **B** Contribution of PCs constituting 95% of variance and 3D score plot. **C** Contributions of individual mass peaks to the segregation of sample groups. *Circled data points* on loading plots indicate statistically significant differences in peak intensities between the groups. The peaks used for PCA calculation are the 50 with the highest signal-to-noise ratio

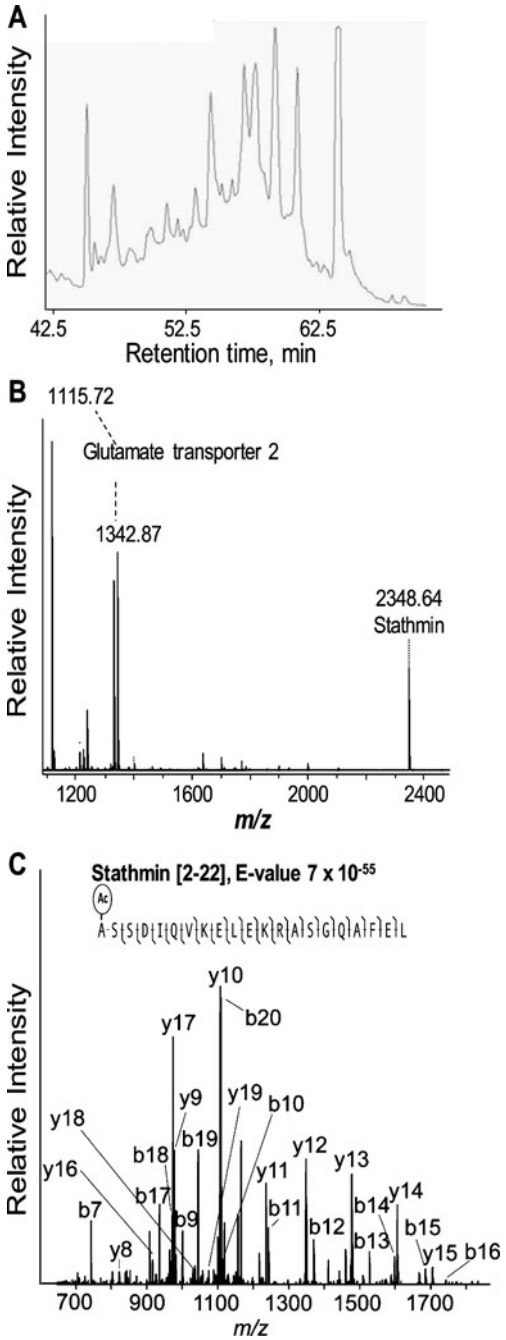

Fig. 6. Identification of peptides by LC-MS. **A** First stage separation by microbore RP-LC. **B** MALDI-TOF MS spectrum of a representative LC fraction used for further peptide sequencing. **C** Fragmentation spectrum shows unambiguous identification of stathmin peptide [2–22]

A total of 74 unique peptides from 28 proteins have been identified by a combination of LC and MS/MS (Table I). Approximately one third of the identified peptides originate from structural myelin-related proteins such as myelin basic protein, myelin oligodendrocyte protein, myelin proteolipid variant sequence, and claudin-11. Claudin-11 is a developmentally regulated protein that belongs to a family of proteins constituting the tight junctions in the brain (35).

Peptides from other structural proteins were also identified, including collagen alpha 2, an endothelial cell-specific protein; neuraxin, a microtubule-associated protein involved in cytoskeletal changes of neurite extension in the rat central nervous system (36,37); and stathmin, a microtubule regulatory protein (38). Many of the identified peptides represent metabolic pathway components; for example, the protein neurogranin, a brain-specific, post-synaptically located substrate of protein kinase C (PKC) from the IQ motif protein family. PKC phosphorylation of neurogranin in animal prefrontal cortex is reported to be affected by antidepressant and psychostimulant drugs (39) that may be involved in synaptic plasticity and spatial learning (40). Peptides from another member of the IQ motif family, neuron-specific polypeptide PEP-19, were also detected. PEP-19 binds to calmodulin through the IQ motif in a Ca^{2+}-independent manner (41) and is thought to exert neuroprotective effects in apoptosis by blocking several calmodulin-dependent pathways. It has been proposed that PEP-19 and neurogranin are involved in regulation of calmodulin (42–44). A growing number of polypeptides/small proteins with the IQ motif and with confirmed calmodulin interactions are thought to regulate important cellular processes, including gene transcription. Also observed was synaptotagmin-11, a calcium-binding protein and a synaptic vesicle, and SNARE component involved in vesicular trafficking and exocytosis.

More than 10% of the identified peptides belong to the neurotransmitter transport-related proteins, among which are glial and neuronal glutamate transporters, regulating synaptic membrane exocytosis protein, histidine triad nucleotide-binding protein 1, and stathmin. The expression of GLT1b in neuronal presynaptic terminals and dendritic shafts, as well as in astrocytes, was previously demonstrated at the mRNA level (45). Sodium- and chloride-dependent GABA transporter 1 (GAT-1, accession P23978) was identified, as was a peptide from synaptotagmin XI, which originates from a membrane-trafficking protein family of calcium sensors for the regulated exocytosis of neurotransmitters, neuropeptides, and hormones (46,47). Synaptotagmins can be induced in the brain after repeated cocaine treatment (48). Many of the energy metabolism-related proteins were identified, such as ATP synthase and fatty acid synthase, Na^+/K^+ ATPase, cytochrome c oxidase, and ATP synthase-coupling factor 6. Finally, approximately 10% of the identified peptides originated from hemoglobin proteins.

Acute Cocaine Exposure Alters a Subset of Peptides in the mPFC and Reveals Peptide Markers of the LCR Phenotype

Which peptides contribute to the observed differences between extracts from control and cocaine-treated samples of the mPFC? We repeated the PCA comparisons for the mPFC samples only and derived peak intensity statistics by paired *t* test. While loading plots in Fig. 4 point to the peaks contributing to spectra classification, *t* test provided a measure of nonrandom association between a particular peak and the observed effect. Thus, statistical analysis of peak intensities following the PCA revealed seven peptides that exhibited changes within a 93% confidence interval ($p=0.07$) between the mPFC sample groups (Table II), among which are acetylated stathmin (P13668) [2-22], acetylated histidine triad nucleotide-binding protein 1 (P62959) [2-42], and a fragment of mitochondrial ATP synthase

Table I. List of Peptides Identified in Pooled Samples of Tissue Extracts from dSTR, NA, and mPFC by LC-MS/MS

Peptide sequence	Mr (calculated)	Protein name	Accession/ID	Mass accuracy, ppm
YSQLQDLV	964.5	Synaptotagmin-11	O08835	−139
KIGGHGGEY	916.4	Hemoglobin subunit alpha-1/2	P01946	209
GKIGGHGGEYG	1,030.5	Hemoglobin subunit alpha-1/2	P01946	147
VSPGSAQVKAHGKKVA	1,562.9	Hemoglobin subunit alpha-1/2	P01946	−133
VVYPWTQR	1,047.6	Hemoglobin subunit beta-1	P02091	33
KVNPDDVGGEA-NH2	1,098.5	Hemoglobin subunit beta-1	P02091	325
VVYPWTQRY	1,210.6	Hemoglobin subunit beta-1	P02091	7
LVVYPWTQRY	1,323.7	Hemoglobin subunit beta-1	P02091	−98
VLLPKKTESHHKAKGK*	1,800.1	Histone H2A type 1	P02262	−12
AVLLPKKTESHHKAKGK*	1,871.1	Histone H2A type 1	P02262	−15
GRGLSLSR	844.5	Myelin basic protein S	P02688	17
DENPVVHF	955.4	Myelin basic protein S	P02688	199
IVTPRTPPPS	1,063.6	Myelin basic protein S	P02688	−57
IVTPRTPPPSQ	1,191.7	Myelin basic protein S	P02688	−69
IVTPRTPPPSQG	1,248.7	Myelin basic protein S	P02688	−83
KDSHTRTTHYG	1,301.6	Myelin basic protein S	P02688	58
PRTPPPSQGKGRG	1,333.7	Myelin basic protein S	P02688	−85
KLGGRDSRSGSPM	1,346.7	Myelin basic protein S	P02688	−55
FKNIVTPRTPPPS	1,452.8	Myelin basic protein S	P02688	48
KSQRTQDENPVVH	1,536.8	Myelin basic protein S	P02688	−60
acASQKRPSQRHGSKY	1,670.9	Myelin basic protein S	P02688	10
KSQRTQDENPVVHF	1,683.8	Myelin basic protein S	P02688	10
*acASQKRPSQRHGSKYL	1,783.9	Myelin basic protein S	P02688	23
SLPQKSQRTQDENPVV	1,824.9	Myelin basic protein S	P02688	24
KSQRTQDENPVVHFF	1,830.9	Myelin basic protein S	P02688	35
acASQKRPSQRHGSKYLA	1,854.9	Myelin basic protein S	P02688	85
IVTPRTPPPSQGKGRGLSL	1,960.1	Myelin basic protein S	P02688	153
SLPQKSQRTQDENPVVH	1,962.0	Myelin basic protein S	P02688	−6
SLPQKSQRTQDENPVVHF	2,109.1	Myelin basic protein S	P02688	−7
SLPQKSQRTQDENPVVHFF	2,256.1	Myelin basic protein S	P02688	27
SLPQKSQRTQDENPVVHFFK	2,384.2	Myelin basic protein S	P02688	11
FSGDRGAPKRGSGKDSHTRT THYGSLPQKSQRTQDENPVVHFF	**4,812.4**	**Myelin basic protein S**	P02688	1
FADKVPKTAENF	1,365.7	Peptidyl-prolyl cis-trans isomerase A	P10111	−157
LQTTATSRRQQEQLVPTLEKFVFT PHVEPECLSESAIL	**4,325.2**	**Fatty acid synthase**	P12785	−4
ASGPGGLPGERGAAGIPGGKGEK GETGLRGEIGNPGRDGARGAP GAIGAPGPAGASG	**5,000.5**	**Collagen alpha 2**	P12785	−6
MIRPKTENL	1,100.6	Na/K ATPase subunit beta-2	P13638	−71
LTISELKPTYQ	1,291.7	Na/K ATPase subunit beta-2	P13638	−28
RVAPPGLTQIPQIQ	1,516.9	Na/K ATPase subunit beta-2	P13638	−32
RVAPPGLTQIPQIQKTE	1,875.1	Na/K ATPase subunit beta-2	P13638	52
DRVAPPGLTQIPQIQKTE	1,990.1	Na/K ATPase subunit beta-2	P13638	55
acASSDIQVKELEKRASGQAFEL	**2,346.3**	**Stathmin**	P13668	2
NKELDPVQKL	1,068.6	ATP synthase-coupling factor 6, mitochondrial	P21571	−51
KELDPVQKL	1,182.7	ATP synthase-coupling factor 6, mitochondrial	P21571	−87
NFEDPKFEVLDKPQS	1,791.9	ATP synthase-coupling factor 6, mitochondrial	P21571	−104
IVRPENGPEQPQAGSSASKEAYI	2,427.2	GABA transporter 1	P23978	−187
YREGKIVQVT	1,191.7	Glial glutamate transporter 1	P24942	−37
SVIEENNEMKKPYQL	1,706.9	Glial glutamate transporter 1	P24942	−56
VPPVQVSPLIKFGRYSALIL	**2,196.3**	**Atp synthase, e chain, mitochondrial**	P29419	1
IRNLFPENL	1,114.6	Glutamate/aspartate transporter 2	P31596	87
IRNLFPENLVQ	1,341.7	Glutamate/aspartate transporter 2	P31596	118
LYRATM	753.4	Cytochrome c oxidase polypeptide 7A2, mitochondrial	P35171	−114
MAAFPKKQN	1,033.5	Cytochrome c oxidase polypeptide 7A2, mitochondrial	P35171	−40

Table I. (continued)

Peptide sequence	Mr (calculated)	Protein name	Accession/ID	Mass accuracy, ppm
LAMAAFPKKQN	1,217.7	Cytochrome c oxidase polypeptide 7A2, mitochondrial	P35171	53
FENKVPEKQKL	1,358.8	Cytochrome c oxidase polypeptide 7A2, mitochondrial	P35171	−24
YTTGAVRQIF	1,154.6	Myelin proteolypid protein	P60203	56
acADEIAKAQVAQPGGDTIF GKIIRKEIPAKIIF	**3,478.0**	**Histidine triad nucleotide-binding protein 1 (Hint1)**	P62959	1
DIPLDDLGANAAAAKIQA	1,749.9	Neurogranin	Q04940	−90
ILDIPLDDPGANAAAAKIQASF	2,210.2	Neurogranin	Q04940	71
RVIGPGHPIR	1,100.7	Myelin oligodendrocyte glycoprotein	Q63345	−48
HAHKLRVDPVNF	1,431.8	Alpha globin	Q63910	11
VHLTDAEKAAVNGL	1,436.8	II beta-globin	Q6LD44	−76
FRKFQKKKAGSQ	1,451.8	PEP-19	Q8CHN7	−148
FRKFQKKKAGSQS*	1,538.9	PEP-19	Q8CHN7	−57
IDMDAPETERAAVAIQSQ	1,943.9	PEP-19	Q8CHN7	−89
DIDMDAPETERAAVAIQSQ	2,059.0	PEP-19	Q8CHN7	−66
PLISS	628.4	Glutamate transporter GLT1b	Q8K5B5	−193
PIHPDVVM	906.5	Glutamate transporter GLT1b	Q8K5B5	−62
AAPIHPDVVM	1,048.5	Glutamate transporter GLT1b	Q8K5B5	−79
GAASIPSAGLVTML	1,286.7	Glutamate transporter GLT1b	Q8K5B5	−316
ISLAEQRLLEDDKRQFDSAWQELM	2,029.4	Vascular endothelial cell specific protein 18	Q91Y80	−13
YYSSGSSSPTHAKSAH	1,764.8	Claudin-11	Q99P82	−62
RSSLGAKMVAI	1,131.6	Regulating synaptic membrane exocytosis protein 3 (RIM 3)	Q9JIR3	132
SLSAASAPLAETSTPL	1,514.8	ProSAAS	Q9QXU9	−108
PPPAPMQDRSPSPRHPDVS	2,067.0	Neuraxin	P15205	−8
74 peptides		**28 proteins**		**−17**

The reported mass is the monoisotopic mass, and mass accuracy represents the differences from the measured and calculated monoisotopic masses. Underlined are residues that are found in order reverse to that of the deposited sequence. Peptides in bold were identified by nanoLC-FT-MS/MS

* Indicates beginning or end of the precursor protein

(P29419) [2-21] identified in the LC-MS/MS experiments. An additional set of peptides further distinguishes profiles from control and cocaine groups with high-loading scores in PCA (Fig. 3) but did not fit into the 90% confidence interval in *t* test. These include LVV-hemorphin-7 and multiple peptides from the glutamate transporters. Although individually, they did not reach the significance threshold, they contribute to a composite effect of acute cocaine exposure for the overall peptide profile observed in the mPFC. In our dataset, eight cocaine-treated animals were designated as either HCRs or LCRs (n=4 for each phenotype) depending on their locomotor score. Comparing the peptide profiles of each of the phenotypes, we found that LCRs, who are more sensitive to cocaine-induced behavioral plasticity and conditioning to the reward-related effects of cocaine, also

Table II. List of Peptides That Are Detected at Significantly Different Intensities in Samples of mPFC from Rats Acutely Treated with 10 mg/kg Cocaine

HCRs + LCRs			LCRs		
n=8			n=4		
Peptide	*P*, *t* test	Ratio [a]	Peptide	*P*, *t* test	Ratio [a]
2168	0.02	1.7	2482	0.07	2
2482	0.02	2			
2198 ATP synthase	0.04	1.7	**2198 ATP synthase**	0.07	1.7
2969	0.04	1.7			
2349 Stathmin	0.04	1.4	**2349 Stathmin**	0.07	1.7
3480 Hint1	0.04	2	**3480 Hint1**	0.07	2.5
3434	0.05	2			

Peptide masses are from the mean spectrum obtained from individual measurements, with the individual spectra being processed as described in the supplemental information

[a] Ratio indicates relative change in peptide signal intensity in the mPFC of cocaine-treated rats, calculated as mean peak intensity in the cocaine-treated group/mean peak intensity in the control group. Peptides in bold were identified by nanoLC-FT-MS/MS

have ~2× more significant increase in peak intensities for the acetylated N terminus peptides of stathmin and Hint 1, as well as truncated ATP synthase, relative to the control group. In contrast, among HCRs, signal intensities of these peptides were elevated, but not significantly (Table II).

DISCUSSION

The neurochemical effects of drugs of abuse have traditionally been studied by focused monitoring of changes in a particular peptide, precursor protein, or mRNA, targeted by selective probes such as antibodies or oligonucleotides (49). We take an alternate route and explore global changes in peptide levels in anatomically defined brain regions to find those that may serve as markers of brain response to acute stimulation with cocaine. Our approach, not limited to a molecule of choice, extends and complements previous studies; it allows a more comprehensive analysis of cocaine-induced biochemical adaptations and provides an opportunity to uncover unexpected interactions. Although MS is not generally considered a quantitative method, we and others have found that precise tissue sampling, optimized spectrum acquisition, and rigorous statistical analysis of the MS data combine to ensure insightful interrogation of biological samples (26,50). The first rapid mass spectrometric profiling of cocaine-treated brain tissue in pooled samples appears to be Geng at al. (23). In that study, two small protein markers were deferentially detected in control and cocaine-treated groups. Likewise, Che and coworkers (51) used MS and found that a total of 10 peptides changed in pooled samples from the prefrontal cortex, hippocampus, striatum, and hypothalamus of $Cpe^{fat/fat}$ mice chronically treated with 10 mg/kg of cocaine. A number of non-candidate studies aided by MS addressed analysis of protein level alterations elicited by psychostimulants. For example, Olausson *et al.* (52) studied the proteome modifications in monkey orbitofrontal cortex related to cognitive motivational impairments in cocaine addiction. Tannu *et al.* analyzed the proteomic alterations in the NAc of cocaine overdose victims (53) and in rhesus monkeys (54) following cocaine self-administration. Mass spectrometric examination of the protein constituents of the NAc in rodent models of morphine abuse revealed changes in structural proteins (55) characteristic of opioid addiction and neurodegenerative diseases in humans (56,57). One of the only proteomics studies to investigate protein changes associated with differing vulnerabilities to cocaine addiction was reported by del Castillo *et al.* (58), who studied a place-conditioning paradigm in behaviorally different subpopulations of rats.

Often in MS-based studies, the effects of psychostimulants are evaluated using samples pooled from multiple animals, with the goal of generating reliably reproducible protein/peptide profiles characteristic of a group trait. While this approach is reasonable, it is difficult to try and establish a relationship between a subject's behavior and neurochemical response using pooled samples. In contrast, profiling individual samples from anatomically defined brain regions alleviates this concern. Furthermore, by reducing the number of processing steps in our extraction protocol, we minimize sample losses and allow small sample sizes. Recognizing that this methodology can make conventional isotopic labeling reactions and LC-MS experiments difficult, we take advantage of the low sample-volume capabilities of direct MALDI MS.

Using this approach, we found that LCRs exhibited increased detection levels of the acetylated N terminus peptides of stathmin and Hint 1, as well as truncated ATP synthase, in the mPFC relative to the control group. The mesocorticolimbic dopaminergic system appears to be involved in many of the neurobiological effects of cocaine (59). While it is generally well accepted that the NAc is involved in cocaine reinforcement, increasing evidence suggests that the mPFC may also play an important role. Cocaine (50–100 pmol in 100 nl) has been self-administered intracranially directly into the mPFC in rats (60,61), but not into the NAc or ventral tegmental area (60), suggesting that this brain region may be involved in the initiation of cocaine reinforcement. Stathmin, a growth-associated protein involved in the regulation of the microtubule filament system, acts by destabilizing microtubules and is involved in the control of learned fear and (62) and anxiety in humans (63). Phosphorylation of stathmin at Ser-16 may be required for axon formation during neurogenesis (38). Stathmin mRNA was previously reported to increase by about 30% in the prefrontal cortex, striatum, NAc, temporal cortex, and hippocampus 0.5–1 h after a single methamphetamine (METH) injection (64). More recently, both stathmin and ATP synthase levels were found to be affected by acute METH administration (65). Changes in the expression of mRNA or protein levels are often reported for various chains of mitochondrial ATP synthase (53,58). In general, mitochondrial function has been reported to be differentially regulated in response to cocaine via decreased protein and/or protein gene expression in the human prefrontal cortex (66). For example, cocaine was shown to activate the mitochondrial apoptotic pathway in cortical neurons (67). Additional markers of LCR phenotype are an unidentified peptide and the acetylated N terminus of Hint1. To our knowledge, Hint1 has not been investigated in detail; thus, its function is yet to be completely determined.

We also found a number of peptides with high-loading scores from PCA that do not show significant differences between cocaine and control animals. Among these are the multifunctional, nonclassical opioid peptides LVV-hemorphin-7, VV-hemorphin-7 (68), and C-terminus-truncated VV-hemorphin-7 of the beta-chain of hemoglobin. As recently reported, hemoglobin alpha and beta are expressed in rat and human central neurons and facilitate oxygen uptake and mediate neuronal response to injury (69,70) as well as interact with peptide receptors (71). Moreover, hemorphins are thought to have therapeutic potential as homeostatic agents in endotoxin-induced stress (72) and have been shown to be released from brain slices in a stimulation-dependent manner (73).

Not surprisingly, most of the peptides identified in this study originate from myelin basic protein (MBP), the most abundant protein component of myelinated fibers in the central nervous system. MBP has a role in both the formation and stabilization of compact myelin and exists in numerous splice forms. Each splice variant and charge isomer may have a specialized function in the assembly and functional properties of myelin membranes. A growing number of reports state that widespread changes to the myelin structure could be associated with the adaptive changes effected by cocaine abuse (74). Exposure to cocaine impairs major components of

myelin, MBP, proteolipid protein, and myelin-associated oligodendrocytic basic protein, which are all decreased in human studies of cocaine abuse (66,75,76). Alteration of myelin structure under chronic cocaine use becomes more evident in newer studies (74,77). More recently, alterations in myelin in the corpus callosum in human cocaine-dependent patients were reported in imaging studies (78). Interestingly, acute amphetamine dosage has been shown to affect degenerative damage of the caudate putamen in rats, manifested by swellings in axons and myelin damage at 4-h post-METH treatment (79). It has been reported, based on microarray analysis studies, that cocaine abusers show a striking decrease in myelin-related genes (75–77,80). Interestingly, few animal studies demonstrating myelin-associated structural or gene expression changes under cocaine have been reported (81). Immunofluorescence analysis showed significant decreases in myelin levels in the rat brain that correlated with the cocaine blood levels (82). Our data provide an additional line of evidence of a connection between factors influencing susceptibility to drug addiction that may interrelate, in part, with myelin integrity in the brain.

CONCLUSIONS

As discussed above, our findings correlate well with the known or suggested changes in metabolism-related and structural protein transcripts or genes following acute cocaine exposure, confirming the broad utility of our label-free, MS-based comparative approach to investigate neurochemical changes. We identified numerous peptides that are potentially targeted in the addiction process, as well as new peptides associated with a higher sensitivity to cocaine.

ACKNOWLEDGMENTS

The project described was supported by Award Numbers DA018310 and DA017940 from the National Institute on Drug Abuse (NIDA). The content is solely the responsibility of the authors and does not necessarily represent the official views of NIDA or the National Institutes of Health. The authors thank Jessica Stanis for technical assistance.

REFERENCES

1. Schuckit MA. Biological, psychological and environmental predictors of the alcoholism risk: a longitudinal study. J Stud Alcohol. 1998;59:485–94.
2. Lambert NM, McLeod M, Schenk S. Subjective responses to initial experience with cocaine: an exploration of the incentive-sensitization theory of drug abuse. Addiction. 2006;101:713–25.
3. Branch CA, Knuepfer MM. Causes of differential cardiovascular sensitivity to cocaine. I: studies in conscious rats. J Pharmacol Exp Ther. 1994;269:674–83.
4. Sabeti J, Gerhardt GA, Zahniser NR. Acute cocaine differentially alters accumbens and striatal dopamine clearance in low and high cocaine locomotor responders: behavioral and electrochemical recordings in freely moving rats. J Pharmacol Exp Ther. 2002;302:1201–11.
5. Saka E, Goodrich C, Harlan P, Madras BK, Graybiel AM. Repetitive behaviors in monkeys are linked to specific striatal activation patterns. J Neurosci. 2004;24:7557–65.
6. Mayfield RD, Larson G, Zahniser NR. Cocaine-induced behavioral sensitization and D1 dopamine receptor function in rat nucleus accumbens and striatum. Brain Res. 1992;573:331–5.
7. Pierce RC, Bell K, Duffy P, Kalivas PW. Repeated cocaine augments excitatory amino acid transmission in the nucleus accumbens only in rats having developed behavioral sensitization. J Neurosci. 1996;16:1550–60.
8. Mantsch JR, Ho A, Schlussman SD, Kreek MJ. Predictable individual differences in the initiation of cocaine self-administration by rats under extended-access conditions are dose-dependent. Psychopharmacology (Berl). 2001;157:31–9.
9. Panlilio LV, Katz JL, Pickens RW, Schindler CW. Variability of drug self-administration in rats. Psychopharmacology (Berl). 2003;167:9–19.
10. Tornatzky W, Miczek KA. Cocaine self-administration "binges": transition from behavioral and autonomic regulation toward homeostatic dysregulation in rats. Psychopharmacology (Berl). 2000;148:289–98.
11. Gulley JM. Individual differences in novelty- and cocaine-induced locomotor activity as predictors of food-reinforced operant behavior in two outbred rat strains. Pharmacol Biochem Behav. 2007;86:749–57.
12. Gulley JM, Hoover BR, Larson GA, Zahniser NR. Individual differences in cocaine-induced locomotor activity in rats: behavioral characteristics, cocaine pharmacokinetics, and the dopamine transporter. Neuropsychopharmacology. 2003;28:2089–101.
13. Mandt BH, Allen RM, Zahniser NR. Individual differences in initial low-dose cocaine-induced locomotor activity and locomotor sensitization in adult outbred female Sprague-Dawley rats. Pharmacol Biochem Behav. 2009;91:511–6.
14. Klein DA, Gulley JM. Reduced sensitivity to the locomotor-stimulant effects of cocaine is associated with increased sensitivity to its discriminative stimulus properties. Behav Pharmacol. 2009;20:67–77.
15. Sabeti J, Gerhardt GA, Zahniser NR. Individual differences in cocaine-induced locomotor sensitization in low and high cocaine locomotor-responding rats are associated with differential inhibition of dopamine clearance in nucleus accumbens. J Pharmacol Exp Ther. 2003;305:180–90.
16. Allen RM, Everett CV, Nelson AM, Gulley JM, Zahniser NR. Low and high locomotor responsiveness to cocaine predicts intravenous cocaine conditioned place preference in male Sprague-Dawley rats. Pharmacol Biochem Behav. 2007;86:37–44.
17. Mandt BH, Schenk S, Zahniser NR, Allen RM. Individual differences in cocaine-induced locomotor activity in male Sprague-Dawley rats and their acquisition of and motivation to self-administer cocaine. Psychopharmacology (Berl). 2008;201:195–202.
18. Stanis JJ, Burns RD, Sherrill LK, Gulley JM. Disparate cocaine-induced locomotion as a predictor of choice behavior in rats trained in a delay-discounting task. Drug Alcohol Depend. 2008;98:54–62.
19. Nelson AM, Larson GA, Zahniser NR. Low or high cocaine responding rats differ in striatal extracellular dopamine levels and dopamine transporter number. J Pharmacol Exp Ther. 2009;331:985–97.
20. Briegleb SK, Gulley JM, Hoover BR, Zahniser NR. Individual differences in cocaine- and amphetamine-induced activation of male Sprague-Dawley rats: contribution of the dopamine transporter. Neuropsychopharmacology. 2004;29:2168–79.
21. Mandt BH, Zahniser NR. Low and high cocaine locomotor responding male Sprague-Dawley rats differ in rapid cocaine-induced regulation of striatal dopamine transporter function. Neuropharmacology. 2010;58:605–12.
22. Abul-Husn NS, Devi LA. Neuroproteomics of the synapse and drug addiction. J Pharmacol Exp Ther. 2006;318:461–8.
23. Geng T, Seitz PK, Thomas ML, Xu B, Soman KV, Kurosky A, *et al.* Use of surface enhanced laser desorption/ionization-time of flight mass spectrometry (SELDI-TOF MS) to study protein expression in a rat model of cocaine withdrawal. J Neurosci Methods. 2006;158:1–12.
24. Kreek MJ. Cocaine, dopamine and the endogenous opioid system. J Addict Dis. 1996;15:73–96.
25. Miura D, Fujimura Y, Tachibana H, Wariishi H. Highly sensitive matrix-assisted laser desorption ionization-mass spectrometry for high-throughput metabolic profiling. Anal Chem. 2009;82:498–504.
26. Uys JD, Grey AC, Wiggins A, Schwacke JH, Schey KL, Kalivas PW. Matrix-assisted laser desorption/ionization tissue profiling of

secretoneurin in the nucleus accumbens shell from cocaine-sensitized rats. J Mass Spectrom. 2010;45:97–103.
27. Li L, Sweedler JV. Peptides in our brain: mass spectrometric-based measurement approaches and challenges. Annu Rev Anal Chem. 2008;1:451–83.
28. Romanova EV, Rubakhin SS, Sweedler JV. One-step sampling, extraction, and storage protocol for peptidomics using dihydroxybenzoic acid. Anal Chem. 2008;80:3379–86.
29. Wilcoxon F. Individual comparisons by ranking methods. Biometrics. 1945;1:80–3.
30. Kruskal WH, Wallis WA. Use of ranks in one-criterion variance analysis. J Am Stat Assoc. 1952;47:588–621.
31. Stephens MA. EDF for goodness of fit and some comparisons. J Am Stat Assoc. 1974;69:730–7.
32. Dudoit S, shaffer JP. Multiple hypothesis testing in microarray experiments. Stat Sci. 2003;18:71–103.
33. Hoteling AJ, Erb WJ, Tyson RJ, Owens KG. Exploring the importance of the relative solubility of matrix and analyte in MALDI sample preparation using HPLC. Anal Chem. 2004;76:5157–64.
34. Shibue M, Mant CT, Hodges RS. Effect of anionic ion-pairing reagent hydrophobicity on selectivity of peptide separations by reversed-phase liquid chromatography. J Chromatogr A. 2005;1080:68–75.
35. Bronstein JM, Chen K, Tiwari-Woodruff S, Kornblum HI. Developmental expression of OSP/claudin-11. J Neurosci Res. 2000;60:284–90.
36. Kirsch J, Littauer UZ, Schmitt B, Prior P, Thomas L, Betz H. Neuraxin corresponds to a C-terminal fragment of microtubule-associated protein 5 (MAP5). FEBS Lett. 1990;262:259–62.
37. Rienitz A, Grenningloh G, Hermans-Borgmeyer I, Kirsch J, Littauer UZ, Prior P, *et al*. Neuraxin, a novel putative structural protein of the rat central nervous system that is immunologically related to microtubule-associated protein 5. EMBO J. 1989;8:2879–88.
38. Watabe-Uchida M, John KA, Janas JA, Newey SE, Van Aelst L. The Rac activator DOCK7 regulates neuronal polarity through local phosphorylation of stathmin/Op18. Neuron. 2006;51:727–39.
39. Szabo ST, Machado-Vieira R, Yuan P, Wang Y, Wei Y, Falke C, *et al*. Glutamate receptors as targets of protein kinase C in the pathophysiology and treatment of animal models of mania. Neuropharmacology. 2009;56:47–55.
40. Gaertner TR, Putkey JA, Waxham MN. RC3/neurogranin and Ca2+/calmodulin-dependent protein kinase II produce opposing effects on the affinity of calmodulin for calcium. J Biol Chem. 2004;279:39374–82.
41. Slemmon JR, Morgan JI, Fullerton SM, Danho W, Hilbush BS, Wengenack TM. Camstatins are peptide antagonists of calmodulin based upon a conserved structural motif in PEP-19, neurogranin, and neuromodulin. J Biol Chem. 1996;271:15911–7.
42. Slemmon JR, Hughes CM, Campbell GA, Flood DG. Increased levels of hemoglobin-derived and other peptides in Alzheimer's disease cerebellum. J Neurosci. 1994;14:2225–35.
43. Gerendasy DD, Herron SR, Watson JB, Sutcliffe JG. Mutational and biophysical studies suggest RC3/neurogranin regulates calmodulin availability. J Biol Chem. 1994;269:22420–6.
44. Smith ML, Johanson RA, Rogers KE, Coleman PD, Slemmon JR. Identification of a neuronal calmodulin-binding peptide, CAP-19, containing an IQ motif. Brain Res Mol Brain Res. 1998;62:12–24.
45. Chen W, Aoki C, Mahadomrongkul V, Gruber CE, Wang GJ, Blitzblau R, *et al*. Expression of a variant form of the glutamate transporter GLT1 in neuronal cultures and in neurons and astrocytes in the rat brain. J Neurosci. 2002;22:2142–52.
46. Gustavsson N, Han W. Calcium-sensing beyond neurotransmitters: functions of synaptotagmins in neuroendocrine and endocrine secretion. Biosci Rep. 2009;29:245–59.
47. von Poser C, Ichtchenko K, Shao X, Rizo J, Sudhof TC. The evolutionary pressure to inactivate. A subclass of synaptotagmins with an amino acid substitution that abolishes Ca2+ binding. J Biol Chem. 1997;272:14314–9.
48. Zhang L, Lou D, Jiao H, Zhang D, Wang X, Xia Y, *et al*. Cocaine-induced intracellular signaling and gene expression are oppositely regulated by the dopamine D1 and D3 receptors. J Neurosci. 2004;24:3344–54.
49. Romanova EV, Hatcher NG, Rubakhin SS, Sweedler JV. Characterizing intercellular signaling peptides in drug addiction. Neuropharmacology. 2009;56:196–204.
50. Hattan SJ, Parker KC. Methodology utilizing MS signal intensity and LC retention time for quantitative analysis and precursor ion selection in proteomic LC-MALDI analyses. Anal Chem. 2006;78:7986–96.
51. Che FY, Vathy I, Fricker LD. Quantitative peptidomics in mice: effect of cocaine treatment. J Mol Neurosci. 2006;28:265–75.
52. Olausson P, Jentsch JD, Krueger DD, Tronson NC, Nairn AC, Taylor JR. Orbitofrontal cortex and cognitive-motivational impairments in psychostimulant addiction: evidence from experiments in the non-human primate. Ann N Y Acad Sci. 2007;1121:610–38.
53. Tannu N, Mash DC, Hemby SE. Cytosolic proteomic alterations in the nucleus accumbens of cocaine overdose victims. Mol Psychiatry. 2007;12:55–73.
54. Tannu NS, Howell LL, Hemby SE. Integrative proteomic analysis of the nucleus accumbens in rhesus monkeys following cocaine self-administration. Mol Psychiatry. 2010;15:185–203.
55. Li KW, Jimenez CR, Schors RCvd, Hornshaw MP, Schoffelmeer ANM, Smit AB. Intermittent administration of morphine alters protein expression in rat nucleus accumbens. Proteomics. 2006;6:2003–8.
56. Lariviere RC, Julien J-P. Functions of intermediate filaments in neuronal development and disease. J Neurobiol. 2004;58:131–48.
57. Ferrer-Alcón M, García-Sevilla JA, Jaquet PE, Harpe RL, Riederer BM, Walzer C, *et al*. Regulation of nonphosphorylated and phosphorylated forms of neurofilament proteins in the prefrontal cortex of human opioid addicts. J Neurosci Res. 2000;61:338–49.
58. del Castillo C, Morales L, Alguacil LF, Salas E, Garrido E, Alonso E, *et al*. Proteomic analysis of the nucleus accumbens of rats with different vulnerability to cocaine addiction. Neuropharmacology. 2009;57:41–8.
59. Koob GF. Drugs of abuse: anatomy, pharmacology and function of reward pathways. Trends Pharmacol. Sci. 1992;13:177–84.
60. Goeders NE, Smith JE. Cortical dopaminergic involvement in cocaine reinforcement. Science. 1983;221:773–5.
61. Stein L, Belluzzi JD. Cellular investigations of behavioral reinforcement. Neurosci Biobehav Rev. 1989;13:69–80.
62. Shumyatsky GP, Malleret G, Shin R-M, Takizawa S, Tully K, Tsvetkov E, *et al*. Stathmin, a gene enriched in the amygdala, controls both learned and innate fear. Cell. 2005;123:697–709.
63. Burkhard B, Klaus-Peter L, Diana A, Dirk AM, Anett M, Alexander S, *et al*. *Stathmin*, a gene regulating neural plasticity, affects fear and anxiety processing in humans. Am J Med Genet B Neuropsychiatr Genet. 2009;153B:243–51.
64. Ujike H, Takaki M, Kodama M, Kuroda S. Gene expression related to synaptogenesis, neuritogenesis, and MAP kinase in behavioral densitization to psychostimulants. Ann N Y Acad Sci. 2002;965:55–67.
65. Li X, Wang H, Qiu P, Luo H. Proteomic profiling of proteins associated with methamphetamine-induced neurotoxicity in different regions of rat brain. Neurochem Int. 2008;52:256–64.
66. Lehrmann E, Oyler J, Vawter MP, Hyde TM, Kolachana B, Kleinman JE, *et al*. Transcriptional profiling in the human prefrontal cortex: evidence for two activational states associated with cocaine abuse. Pharmacogenomics J. 2003;3:27–40.
67. Cunha-Oliveira T, Rego AC, Cardoso SM, Borges F, Swerdlow RH, Macedo T, *et al*. Mitochondrial dysfunction and caspase activation in rat cortical neurons treated with cocaine or amphetamine. Brain Res. 2006;1089:44–54.
68. Garreau I, Zhao Q, Pejoan C, Cupo A, Piot JM. VV-hemorphin-7 and LVV-hemorphin-7 released during *in vitro* peptic hemoglobin hydrolysis are morphinomimetic peptides. Neuropeptides. 1995;28:243–50.
69. Richter F, Meurers BH, Zhu C, Medvedeva VP, Chesselet MF. Neurons express hemoglobin alpha- and beta-chains in rat and human brains. J Comp Neurol. 2009;515:538–47.
70. Schelshorn DW, Schneider A, Kuschinsky W, Weber D, Kruger C, Dittgen T, *et al*. Expression of hemoglobin in rodent neurons. J Cereb Blood Flow Metab. 2009;29:585–95.
71. Murillo L, Piot JM, Coitoux C, Fruitier-Arnaudin I. Brain processing of hemorphin-7 peptides in various subcellular fractions from rats. Peptides. 2006;27:3331–40.

72. Barkhudaryan N, Zakaryan H, Sarukhanyan F, Gabrielyan A, Dosch D, Kellermann J, *et al*. Hemorphins act as homeostatic agents in response to endotoxin-induced stress. Neurochem Res. 2009. doi:10.1007/s11064-009-0097-3
73. Annangudi SP, Luszpak AE, Kim SH, Ren S, Hatcher NG, Weiler IJ, *et al*. Neuropeptide release is impaired in a mouse model of fragile-X mental retardation syndrome. ACS Chem Neurosci. 2010;1:306–14.
74. Kristiansen LV, Bannon MJ, Meador-Woodruff JH. Expression of transcripts for myelin related genes in postmortem brain from cocaine abusers. Neurochem Res. 2009;34:46–54.
75. Albertson DN, Pruetz B, Schmidt CJ, Kuhn DM, Kapatos G, Bannon MJ. Gene expression profile of the nucleus accumbens of human cocaine abusers: evidence for dysregulation of myelin. J Neurochem. 2004;88:1211–9.
76. Bannon M, Kapatos G, Albertson D. Gene expression profiling in the brains of human cocaine abusers. Addict Biol. 2005;10:119–26.
77. Sokolov BP. Oligodendroglial abnormalities in schizophrenia, mood disorders and substance abuse. Comorbidity, shared traits, or molecular phenocopies? Int J Neuropsychopharmacol. 2007;10:547–55.
78. Moeller FG, Hasan KM, Steinberg JL, Kramer LA, Valdes I, Lai LY, *et al*. Diffusion tensor imaging eigenvalues: preliminary evidence for altered myelin in cocaine dependence. Psychiatry Res. 2007;154:253–8.
79. Bowyer JF, Robinson B, Ali S, Schmued LC. Neurotoxic-related changes in tyrosine hydroxylase, microglia, myelin, and the blood-brain barrier in the caudate-putamen from acute meth-amphetamine exposure. Synapse. 2008;62:193–204.
80. Albertson DN, Schmidt CJ, Kapatos G, Bannon MJ. Distinctive profiles of gene expression in the human nucleus accumbens associated with cocaine and heroin abuse. Neuropsychopharma-cology. 2006;31:2304–12.
81. Lull ME, Freeman WM, Vrana KR, Mash DC. Correlating human and animal studies of cocaine abuse and gene expression. Ann N Y Acad Sci. 2008;1141:58–75.
82. Narayana PA, Ahobila-Vajjula P, Ramu J, Herrera J, Steinberg JL, Moeller FG. Diffusion tensor imaging of cocaine-treated rodents. Psychiatry Res. 2009;171:242–51.